Journal of Polymers and the Environment (2023) 31:5462–5476
https://doi.org/10.1007/s10924-023-02956-1

ORIGINAL PAPER

Control of Biodegradability Under Composting Conditions and Physical Performance of Poly (Lactic Acid) Based Materials Modified with Phenolic-Free Rosin Resin

Harrison de la Rosa-Ramírez[1] · Miguel Aldas[2] · José Miguel Ferri[1] · Franciszek Pawlak[1] · Juan López-Martínez[1] · María Dolores Samper[1]

Accepted: 6 June 2023 / Published online: 4 July 2023

Abstract
Biodegradable materials based on poly (lactic acid) (PLA) and a phenolic free modified rosin resin were obtained and studied to control the biodegradability under composting conditions of the materials. The resin was blended in concentrations of 1, 3, 5, 10, and 15 parts per hundred (phr) of base polymer using industrial plastic processing techniques. Additionally, to study the effect of the resin on the compatibility of the PLA, the physical performance, water absorption, mechanical behavior, thermal stability, and microstructure of the materials were assessed. The resin incorporation decreased the resistance to thermal degradation of the resultant material, and the composting disintegration rate was slowed down with the increasing content of the resin. The water diffusion was delayed, and the diffusion and corrected diffusion coefficients decreased with the rising content of UP. The mechanical properties tend to decrease while a saturation effect was observed for contents higher than 3 phr of resin. The optimal amount of resin that can be added to achieve good interaction with PLA matrix, complete miscibility, and good material cohesion is 3 phr.

Keywords Gum rosin derivative · UP resin · Poly (lactic acid) · Biodegradability · Phenolic free rosin resin

Introduction

Global concern about the amount of polymeric waste material generated in recent decades is growing. Although government institutions promote the circular economy and recycling policies, much of the polymeric waste derived from post-consumption is in landfills, rivers, and even oceans in many other cases, causing an environmental imbalance. It should be kept in mind that recycling these polymers is a good alternative, but more is needed since a large number of plastic products are single-use [1]. Biodegradable or bioplastic polymers are an excellent alternative to traditional polymers for this type of single-use product [2, 3].

Currently, the consumption of bioplastics is approximately 1% compared to the quantity of commercial plastic produced worldwide. However, the demand for bioplastics is expected to increase in the coming years, even after stagnating in 2020 because of Covid-19. The market concerns especially polylactic acid (PLA), which production capacity is estimated to increase by 80% by 2027, according to data collected by European Bioplastics in cooperation with Nova-Institute of Research [4].

PLA is one of the most interesting biopolymers to be used as a substitute for petroleum-based polymers, in applications with a short life cycle, due to its relatively short decomposition time under composting and hydrolytic disintegration conditions [5, 6]. Besides its commercial availability at an affordable price (2.80–3.20 €/kg, data obtained in 2023) and the versatile characteristics that make it suitable to be transformed by most of the conventional plastics processing methods (extrusion, injection molding, blow molding, biaxial-oriented films manufacturing, and other) [7–9]. PLA is a biodegradable and biobased linear polyester that is synthesized by polymerization from sugars obtained from biomass (such

✉ Harrison de la Rosa-Ramírez
hardela@epsa.upv.es; harrison.dr@hotmail.com

[1] Instituto de Tecnología de Materiales (ITM), Laboratorio C1L2, Universitat Politècnica de València (UPV), Plaza Ferrándiz y Carbonell 1, 03801 Alcoy, Alicante, Spain

[2] Departamento de Ciencia de Alimentos y Biotecnología, Facultad de Ingeniería Química y Agroindustria, Escuela Politécnica Nacional, 170517 Quito, Ecuador

as sugar cane or corn), mainly by ring-opening polymerization (ROP) of lactic acid obtained in the fermentation of biomass [10]. Compared with other biopolymers, PLA possesses a high rigidity, low elongation at break (of about 5%) [11, 12], and low water and oxygen permeability [13, 14]. Research in different directions is carried out to try to overcome these drawbacks and improve the physical properties of PLA. On the one hand, copolymerization with other biopolymers can be carried out [15, 16], but more economically viable solutions exist. On the other hand, PLA plasticization could be carried out using vegetable oil derivatives such as epoxidized cottonseed oil (ECSO), epoxidized fatty acid esters, epoxidized Karanja oil (EKO) [17–20] and blending with other biopolymers such as thermoplastic starch [21, 22], polyhydroxyalkanoates (PHAs) [23, 24], poly (ε-caprolactone) (PCL) [25, 26].

In addition, some polymers derived from petroleum resource has been used to provide ductility to PLA, such as polyethylene terephthalate (PET) [27], polyvinyl chloride (PVC) [28], and polyethylene (PE) [29, 30]. Blending is one of the most feasible options in polymer mixtures' preparation methods since it combines profitability with a balance in the properties obtained.

It should be noted that it is preferable to blend PLA with other biodegradable polymers since, otherwise, it could lose one of the intrinsic properties of PLA, its biodegradability. One of many particularities of PLA degradation involves the need for a controlled or particular environmental condition to be effective, as is the case of enzymatic degradation and the degradation under composting. Some authors state that PLA biodegradation begins on the material's surface and rapidly spreads into the whole structure [31].

This statement relates well to the combined factors of degradation under composting conditions. On one side is the chemical and/or enzymatic hydrolysis, and on the other is the action of the microorganisms that coexist in the aerobic reactor compost [32, 33]. Due to the action of microorganisms, lactide acid is digested. Therefore, PLA is mainly decomposed into water and organic material. In this basic, the possibilities of modifying some properties by incorporating additives from natural origin should be remembered since it allows respecting the bio-based commitment and biodegradable properties of PLA. In this sense, rosin was used to provide antibacterial properties to PLA/PBAT blends [34]. The natural resin of pine trees, gum rosin, can give a plasticity effect, enhance the biodegradability of PLA [35] and increase its melt flow index [36], which allows, with slight modifications of the resin and adjusting the quantities added, the improvement of PLA properties for its use in different applications and its transformation by various processing techniques. Another aspect that may be of interest to be controlled is the degree of biodegradability, according to the lifetime of the final products. In this sense, small amounts of fumaric acid can be used to control the hydrolysis process of PLA, making it more durable [37].

To enhance rosin resin properties, they are often modified with alkyl phenols or formaldehyde, among others. However, some modifications are not desired due to human health risks and increasing environmental awareness. New alternative approaches of phenol-free modifications are currently being studied, such as ones based on acrylic acid or maleic anhydride. Unik Print 3340 (UP) is a solid amorphous phenolic-free modified rosin resin primarily used in ink production and manufacturing of road marking products. Due to the adhesive and tack behavior in the hot melt state, besides the intrinsic hydrophobic and antibacterial characteristics of pine trees resin and its derivatives, these natural products could be used as an additive for PLA to modify some of its properties, such as brittleness excess and control the hydrolysis during degradation to obtain more durable products. Considering all these points, this study was proposed to control the biodegradability of the PLA and the phenolic-free modified rosin resin blends under composting disintegration conditions.

For this reason, UP was added at different concentrations to the PLA matrix and processed by industrial-level processing techniques (extrusion blending and injection molding). To study the effect of the rosin additive on the compatibility between both components, the physical performance, the mechanical behavior, the thermal stability, the microstructure, and the disintegrations under controlled composting conditions of the final materials were studied.

Experimental

Materials

Polylactic acid (PLA) Purapol LX175, obtained from Corbion Purac (Amsterdam, Netherlands), was used as a thermoplastic matrix. This commercial grade is characterized by having a 96% of L-isomer, a density of 1.24 g cm^{-3}, and a melt flow rate (MFR) of 8 g/10 min (210 °C, 2.16 kg). To prepare the binary compound formulations, a phenolic-free modified rosin resin was used under the trade name Unik Print 3340 (UP), kindly supplied by United Resins—Produção de Resinas S. A (Figueira da Foz, Portugal). UP is a maleic anhydride and fumaric acid modified-rosin resin with a softening point of 135 °C, acid value <35 mL KOH/g, and viscosity in the range of 15–30 Pa·s (23 °C, 25 s^{-1}).

Binary Blend Compound Preparation

For better handling, UP was used in powder form. It was ground by hand using a porcelain mortar and then processed in an RP09 CISA® (Barcelona, Spain) sieve shaker to obtain the

powder (maximum particle size of 250 µm). Before material processing, PLA pellet and UP powder were stored for 12 h at 50 °C in a dehumidifier oven model D-82152 from MMM Medcenter GmbH (München, Germany) to reduce the moisture and avoid PLA degradation during the extrusion process (since PLA is susceptible to hydrolytic degradation). Subsequently, PLA and UP powder were dosed into a compounder twin-screw extruder (25 L/D ratio) Haake Rheocord 9000 system torque (Karlsruhe, Germany) to obtain a homogeneous blended material. PLA was dosed by a K-QX2 single-screw gravimetric feeder from K-Tron GmbH (Niederlenz, Switzerland), while UP powder was dosed by a K-SFS-24 twin-screw gravimetric powder feeder, from K-Tron GmbH (Niederlenz, Switzerland). The profile temperature program for the extrusion process was 60, 160, 165, 170, 175, 180, and 180 °C (from the feed hopper to the material outlet nozzle), with a selected screw speed of 20 rpm. The extruded materials were cooled in a water bath at 20 °C and pelletized using a Haake D-76227 rotary knife unit (Karlsruhe, Germany). Blends were designated as described in Table 1. Before obtaining the testing specimens for characterization (dumbbell shape "1BA" and rectangular specimens 80 × 10 × 4 mm^3), the pellets were dried for 12 h at 50 °C in a dehumidifier oven model MDEO from Industrial Marsé (Barcelona, Spain), then processed using a Sprinter 11t injection machine from Erinca S.L (Barcelona, Spain) with the temperature profile of 175 °C (chamber) and 185 °C (injection nozzle), filling and cooling time set on 2 and 30 s, respectively.

Thermal Analysis

The thermal degradation was studied using thermogravimetric analysis (TGA). The thermogravimetric analysis (TGA) was carried out in a Linseis TGA PT1000 (Selb, Germany), placing an average sample weight of 15 mg in standard alumina crucibles (70 µL). The test was conducted from room temperature (25 °C) to 700 °C, at a heating rate of 10 °C min^{-1}, in an inert nitrogen atmosphere (30 mL min^{-1}). The main thermal transitions of the processed materials were determined using a differential scanning calorimeter (DSC) from Mettler-Toledo 821 equipment (Schwerzenbach, Switzerland). DSC analyses were done in two different conditions to evaluate its behavior.

Condition 1: programmed in three dynamic thermal cycles; initial heating from 25 to 180 °C, then cooling from 180 to −50 °C, and a second heating cycle from −50 to 350 °C, were employed. The average sample weight was 6 mg placed into 40 µL standard aluminum crucibles, with a heating–cooling rate of 10 °C min^{-1}.

Condition 2: it was programmed with the same three dynamic thermal cycles indicated in condition 1. However, the tests were performed at a heating–cooling rate of 5 °C min^{-1}. The degree of crystallinity (X_c) of the samples was calculated using the following Eq. 1:

$$X_C = \left[\frac{\Delta H_m - \Delta H_{cc}}{\Delta H_m^0 \times (1-w)}\right] \times 100 \quad (1)$$

where ΔH_m is the melting enthalpy (Jg^{-1}), ΔH_{cc} is the cold crystallization enthalpy (Jg^{-1}), ΔH_m^0 represents the theoretical melting enthalpy of a full crystalline PLA i.e. 93.0 (Jg^{-1}) [38] and $(1 - w)$ correspond to the weight fraction of PLA in the samples. As formulations were prepared in parts per hundred (phr), the PLA quantity was normalized to the corresponding weight fraction for each formulation.

Disintegration Under Controlled Composting Conditions

The disintegration rate under controlled composting conditions of PLA, UP resin, and PLA-UP mixtures was performed by following the guidelines of ISO-20200 standard. Wet synthetic compost was prepared by mixing 40% sawdust, 10% mature compost, 30% rabbit food, 10% corn starch, 5% sugar, 4% corn oil, and 1% urea. Additionally, it was mixed with water in a 45:55 ratio. Samples sizing 25 × 25 × 1 mm^3 were prepared in an MP170 manual hydraulic heat press machine (160 °C for PLA and PLA-UP mixtures and 100 °C for the UP resin samples). After, they were dried at 50 °C for 48 h in a dehumidifier oven model MDEO. Then, each sample was weighed in an AG245 analytical balance from Mettler Toledo Inc. (Schwerzenbach, Switzerland) and contained in a textile mesh to allow easy removal from the compost and the moisture and microorganism access.

Subsequently, all samples were buried at about 5 cm depth in a perforated plastic box reactor (300 × 200 × 100 mm^3) containing the wet synthetic compost. All samples were immersed in distilled water before being placed into the aerobic compost. To guarantee the aerobic conditions, the reactor was introduced in an air-circulating oven at 58 °C for 91 days, and the wet synthetic compost was periodically mixed according to the ISO-20200 standard. One sample of each formulation (PLA-UP mixtures and PLA) was extracted from the disintegration reactor at 3, 7, 14, 21, 28, 35, 42, 49, and 56 days of the test;

Table 1 Composition of the formulated materials and labeling

Polymeric matrix	Resin derivative	Resin content (phr)					
		0	1	3	5	10	15
PLA	UP3340 (UP)	PLA	PLA-1UP	PLA-3UP	PLA-5UP	PLA-10UP	PLA-15UP

while UP resin samples were extracted at 3, 7, 14, 21, 28, 35, 49, 63, 70, 77, 84 and 91 days of composting. After the extraction, samples were gently cleaned with distilled water, dried in an oven at 40 °C for 24 h, and reweighed. To evaluate the disintegration degree (*D*), the weight of the samples was normalized, at different days of incubation, to the initial weight using Eq. 2. In addition, the evolution of the disintegration process was evaluated by a series of optical images taken from each sample after the extraction from the reactor.

$$D = \left[\frac{W_i - W_r}{W_i}\right] \times 100 \tag{2}$$

where W_i is the initial dry mass of the test material, and W_r is the dry mass of residual test material recovered from sieving.

Water Absorption Study

The water absorption evaluation was performed under soaking conditions by immersing rectangular shape testing specimens ($80 \times 10 \times 4$ mm^3) into distilled water (at 23 ± 1 °C). Before the soaking test, all samples were dried at 50 °C for 24 h; then, cooled to room temperature, and right after, initial samples weight (m_0) was measured using an electronic AG245 analytical balance from Mettler Toledo Inc. (Schwerzenbach, Switzerland) with a precision of ±0.1 mg. The evolution of water absorption was followed periodically by taking out the samples and removing the residual water from their surface with secant paper and then measuring the wet weight (m_1). This procedure was repeated for 15 weeks, setting the weight changes assessment periods every 1 h during the first 10 h of immersion. Then, it was increased to every 24 h until completing the first week of immersion, and then, a weight change assessment was established weekly. The materials' water absorption ($M_{\%}$) was calculated by using Eq. 3:

$$M_{\%} = \left[\frac{W_t - W_0}{W_0}\right] \times 100 \tag{3}$$

where W_t is the weight after a specific t immersion time, and W_0 corresponds to the initial weight of the dry sample before immersion.

From the water absorption data, in specific from the saturation weight (W_s), estimated in the linear region of the weight gain graph, ISO 62:2008 allows the application of Fick's first law to determine the diffusion coefficient (*D*) by using Eq. 4 [39–41]:

$$\frac{W_t}{W_s} = \frac{4}{d}\left(\frac{Dt}{\pi}\right)^{\frac{1}{2}} \tag{4}$$

where *D* is the diffusion coefficient, *d* is the initial thickness of the sample (mm), and W_s is the saturation weight in the linear region.

A graph representation of W_t/W_s versus $t^{1/2}$ permits an estimation of the diffusion coefficient by calculating the slope (θ). Therefore, the diffusion coefficient (*D*) can be determined by following Eq. 5:

$$D = 0.0625\pi d^2\theta^2 \tag{5}$$

where *d* is the initial thickness of the sample (mm), and θ is the slope of W_t/W_s versus the $t^{1/2}$ graph. Equation 5 is valid for the diffusion coefficient calculation of films since it is a one-dimensional shape. However, Eq. 6 considers different corrections to make this equation suitable for three-dimensional shapes [40].

$$D_c = \left(1 + \frac{d}{h} + \frac{d}{w}\right)^{-2} \tag{6}$$

where *Dc* is the corrected diffusion coefficient, considering the three-dimensional geometry, *h* is the total length (mm), *w* is the width (mm), and *d* is the sample thickness (mm). This equation assumes that the diffusion rates are the same for all directions [5, 42].

Mechanical Properties

Mechanical properties of PLA and PLA-UP mixtures were assessed by tensile tests following the guidelines of ISO 527, using an Ibertest electromechanical universal testing machine model ELIB 30 (Madrid, Spain), equipped with a 5 kN load cell. The tensile tests were performed at a speed rate of 10 mm min^{-1}. Moreover, the Charpy impact resistance and hardness of the processed materials were studied. The energy absorption of the materials was determined using a 6J Charpy pendulum in an impact test machine from Metrotec, S. A (San Sebastián, Spain), under ISO 179 standards. Five specimens were employed for the tensile and impact resistance tests, respectively. The Shore D hardness was measured in triplicates under the guidelines of ISO 868, at room conditions (24 °C and relative humidity of 35%), using a durometer 676-D from Instruments J. Bot SA (Barcelona, Spain). In all the tests, the mean and the standard deviation are reported.

In addition, a dynamic mechanical, thermal analysis (DMTA) in torsion mode was performed on the PLA-UP blends, carried out on an AR G2 oscillating rheometer from TA Instruments (New Castle, USA). Specific clamps were adapted for fastening the tested specimens (approximate dimensions of $40 \times 10 \times 4$ mm^3). Tests were performed from 30 to 130 °C, at a heating rate of 2 °C min^{-1}, with a frequency of 1 Hz and a maximum deformation (γ) of 0.1%.

Morphological Study

The microstructure of the cross-section of the broken impact test specimens was observed and characterized by a field

emission scanning microscope (FESEM), using a microscope ZEISS ULTRA 55 from Oxford Instruments (Oxfordshire, United Kingdom) operated at 2 kV. Before observation, all samples were coated with a gold–palladium alloy to increase their surface conductivity on a Sputter Coater Emitech SC7620, Quorum Technologies (East Sussex, UK).

Results and Discussion

Thermal Degradation and Thermal Characterization of PLA-UP Blends

Thermogravimetric analysis (TGA) was used to evaluate the weight reduction and thermal stability of the PLA-UP mixtures. Figure 1 shows the plot comparison of thermogravimetric (TGA) and derivative thermogravimetric (DTG) curves obtained by the TGA technique. It also shows the onset degradation temperatures ($T_{5\%}$, temperature at 5% of mass loss) and the temperatures of the maximum decomposition rate (T_{max}, calculated from the first derivative of the DTG curves. In Fig. 1a, the single degradation step that characterizes PLA can be observed, with a $T_{5\%}$ around 341.7 °C, a similar value to those formerly reported by other studies [43–45].

It can also be observed that the other TGA curves, corresponding to PLA-UP mixtures, are placed more to the left side if compared to the neat PLA TGA curve. To this fact, it is evident that the degradation process of PLA-UP mixtures occurs at lower temperatures. Even though the $T_{5\%}$ of PLA-UP mixtures remains at high values (~340 °C) for UP content equal to or lower than 3 phr, it was observed that, beyond this content, it remarkably reduced the $T_{5\%}$ to lower values, dropping up to 294 °C for PLA with 15 phr UP content, about 47 °C of difference compared to neat PLA ($T_{5\%}$ = 341.7 °C). These earlier mass loss of the PLA-UP mixtures, compared to neat PLA, could be explained due to the beginning of UP molecules degradation, which is also manifested in the appearance of small peaks in the DTG curves around 330 °C, as shown in Fig. 1b, which are related to the degradation of some components of the UP molecules (fumaric acid) [37], in good accordance with the $T_{5\%}$ of UP resin, as shown in Fig. 2a. According to the T_{max}, UP resin degrades at higher temperatures than PLA, as shown in Fig. 2 (PLA T_{max} = 370.8 °C, UP T_{max} = 410.5 °C). However, when UP is added into PLA in the content above 10 phr, the beginning of the resin degradation causes a considerable reduction in the T_{max}, about 5 and 10 °C for the PLA-10UP and the PLA-15UP, respectively.

According to previous studies, the thermal degradation of PLA depends on the hydroxyl groups at the end of its chain, which is associated with non-radical cleavage and intermolecular transesterification due to the susceptibility of ester groups to thermal degradation [46–48]. In this study, the reduction of PLA thermal stability could be explained by the fact that UP resin addition decreases the activation energy of the transesterification reaction, inducing it to happen at lower temperatures and, therefore, encouraging the PLA chain scission when UP resin is added in content equal or higher than 5 phr. In previous work, Valentina et al. [37] reported that fumaric acid enhances the thermal stability of PLA, increasing its onset degradation temperature by more than 20 °C with only a 1% addition. However, the addition of UP to PLA led to a contrary effect. It must be considered that even though UP is a fumaric acid-modified rosin resin, UP resin contains other components (such as maleic anhydride adduct) that could increase PLA thermal degradation.

The main thermal parameters obtained by DSC of PLA-UP mixtures were taken from the curves of the second heating cycle and are shown in Table 2 and Fig. 3. As can be

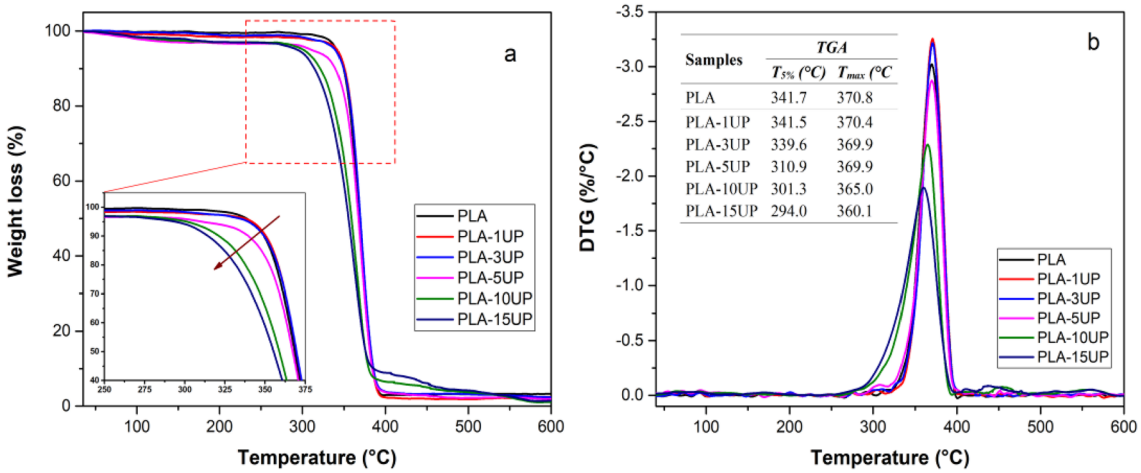

Fig. 1 Comparative TGA (**a**), and DTG (**b**) curves of PLA-UP mixtures

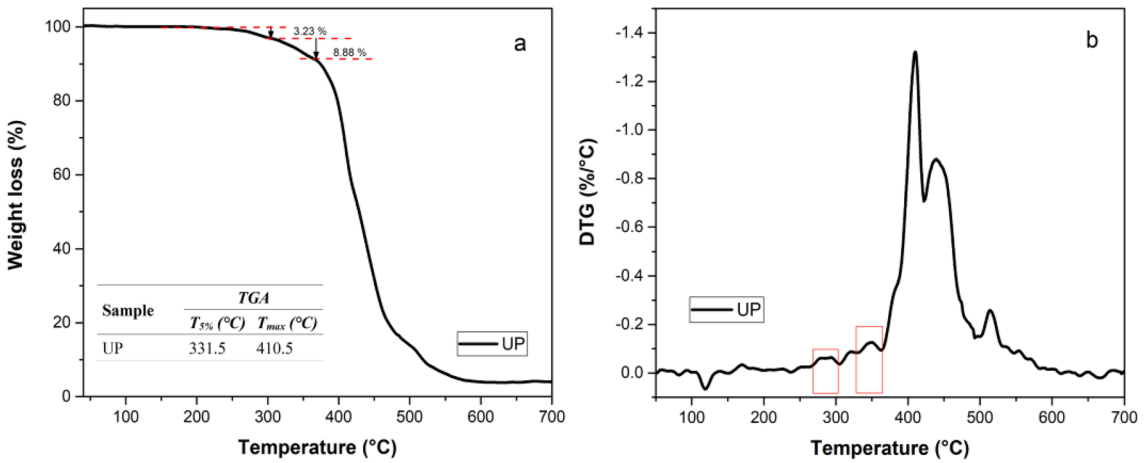

Fig. 2 TGA (**a**), and DTG (**b**) curves of UP resin

Table 2 Main thermal transition values of PLA and PLA-UP mixtures, obtained from the differential scanning calorimetry (DSC) second heating cycle, performed at a speed rate of 10 °C min^{-1} and 5 °C min^{-1}, respectively

Samples	DSC results (at a speed rate of 10 °C min^{-1})						DSC results (at a speed rate of 5 °C min^{-1})					
	T_g (°C)	T_m (°C)	ΔH_m (Jg^{-1})	T_{cc} (°C)	ΔH_{cc} (Jg^{-1})	X_c (%)	T_g (°C)	T_m (°C)	ΔH_m (Jg^{-1})	T_{cc} (°C)	ΔH_{cc} (Jg^{-1})	X_c (%)
PLA	62.2	159.8	33.5	129.5	27.8	6.1	60.5	158.7	32.5	124.1	26.6	6.3
PLA-1UP	61.9	157.1	32.5	124.8	29.4	3.4	60.6	157.8	32.9	119.3	29.0	4.2
PLA-3UP	62.0	157.6	3.4	132.3	2.1	1.4	60.3	156.0	33.5	122.3	32.1	1.5
PLA-5UP	61.7	157.0	1.1	132.8	0.5	0.7	60.4	156.9	12.8	130.9	12.0	0.9
PLA-10UP	61.2	157.0	1.2	133.0	0.7	0.6	60.2	156.6	7.5	131.1	6.9	0.7
PLA-15UP	61.4	157.0	2.2	134.1	1.8	0.4	60.0	156.4	12.1	131.4	11.7	0.5

observed, a glass transition temperature (T_g) value of about 62 °C was obtained for neat PLA, related to the transition of amorphous regions of the polymer to a more flexible and rubbery state. The thermal parameters associated with the phase transition that characterize thermoplastic semi-crystalline materials, cold crystallization temperature (T_{cc}), and melting temperature (T_m) were also clearly identified for neat PLA. Due to the packing and rearrangement of the neat PLA polymer chains, the cold crystallization process occurred at around 130 °C, and its melting temperature was at ~160 °C. For PLA-UP mixtures, no significant change was observed in the T_g values since the baseline steps associated with this thermal phenomenon remained in a temperature range from 61.2 to 62.2 °C (1 °C of difference), as shown in Table 2 and Fig. 3. However, it was observed that the incorporation of UP resin to the PLA noticeably reduced the cold crystallization enthalpy (ΔH_{cc}) values, as the area of the exothermic peak became smaller up to gradually disappear the crystallization peaks with the increasing content of UP resin, indicating a very low crystallization rate of the PLA, except for the mixture with 1 phr content of UP resin. For neat PLA, a ΔH_{cc} value of 27.8 Jg^{-1} was obtained; meanwhile, adding

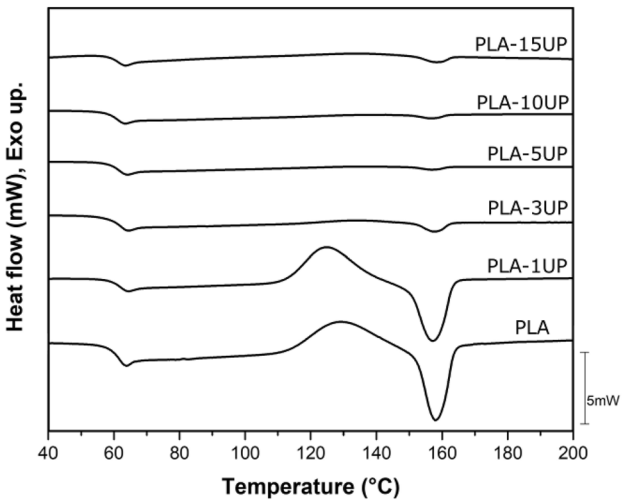

Fig. 3 Differential scanning calorimetry (DSC) curves, second heating cycle at a speed rate of 10 °C min^{-1}, of PLA and PLA and PLA-UP mixtures

3 and 5 phr of UP, the ΔH_{cc} values were 2.1 and 0.5 Jg^{-1}, respectively. A similar effect was formerly observed on PLA/ based composites, as reported by Quiles-Carrillo et al. [7] who suggested that the poorly defined T_{cc} peaks could be ascribed to a rupture of the crystalline structure of PLA.

Furthermore, increasing UP resin content beyond 1 phr gradually shifted the T_{cc} peaks to higher temperatures. These results suggest that the higher the UP content is in the PLA matrix, the more complex the crystallization phenomenon is to occur due to aromatic groups present in UP resin may act as a steric hindrance (causing a steric hindrance effect [49]) to PLA molecular chains by preventing their rearrangement. The higher value of $T_{cc}$was obtained for the mixture with 15 phr content of UP resin (134.1 °C), a percentage increment of about 22%. However, incorporating 1 phr content of UP resin slightly decreased the T_{cc} value to 124.8. This behavior is assumed to be ascribed to a plasticizing effect provided by UP resin in this low content, which is insufficient to produce the steric hindrance effect. Instead, it allows the crystallization nuclei to continue growing. Hence, a relatively high crystallinity degree (X_c) is still observed (3.4%). Nevertheless, it was already lower than neat PLA (6.1%) and gradually reduced to 0.4% for the mixture with 15 phr of UP resin.

To corroborate the effect of steric hindrance, the analyzes were performed at 5 °C min^{-1}. This new assessment allowed us to refute that the crystallization process of PLA could have been promoted to a lower cooling rate. Although, this is well known by the scientific community since there is more time for the chains to be ordered. Only the T_{cc} values shift to lower temperatures. However, neither the ΔH_{cc} nor the X_c has changed. Therefore, it can be concluded that the steric hindrance effect exerted by the UP resin is corroborated.

Disintegration Under Controlled Composting Conditions of PLA-UP Mixtures

Since PLA is considered a biodegradable polymer due to its inherent sensibility of the ester linkages on its structure to enzymatic and chemical hydrolysis [50], it was evaluated the effect of the incorporation of UP resin on the biodegradable characteristics of the mixtures to understand better the interaction between UP resin and PLA matrix, as well as evaluate the influence of the natural resin derivative (with the hydrophobic character) over the chemical hydrolysis of PLA during the disintegration process.

Figure 4 shows the visual appearance of the samples of UP resin, neat PLA, and PLA-UP mixtures after different incubation times under controlled composting conditions. At the beginning (day 0, before being placed into the disintegration reactor), UP resin is characterized by having a shiny yellow tone, PLA is well known for its intrinsic transparency aspect, and PLA-UP mixtures have a distinctive characteristic from whitish to yellowish color (with the increasing UP resin content). It is well known that PLA degradation primarily begins due to the autocatalytic hydrolysis reaction of the ester linkages along its backbone, which causes the loss of transparency of the polymer, making it opaque and whitish [50], as it is observed in the PLA sample after 3 days of incubation. Similar behavior was observed for PLA mixture with 1 phr of UP resin content. Meanwhile, samples with more than 3 phr of UP resin content did not show significant changes in appearance after 3 days of incubation. Still, after 7 days of the test, these samples showed color differences due to the mentioned hydrolysis reaction. Next, neat PLA and its mixtures with lower content of UP resin (1 and 3 phr) became breakable after 14 days in compost, evidenced by the slight cracks observed on the surface of the samples. After 28 days, they started to fall apart into small pieces. On the contrary, it is not until the 21 days when samples with the highest content of UP (5, 10, and 15 phr) start to show cracks on their surfaces, which spread throughout the samples until causing their separation into small pieces at the end of the disintegration period (from day 35 to day 56). In previous work, Pantani et al. [51] reported that amorphous regions of PLA seem more easily accessible by enzymatic attacks. In the present study, it was confirmed by the DSC technique that PLA-UP mixtures become more amorphous with the increasing content of UP resin. Therefore, a higher disintegration rate for PLA-UP mixtures could be expected along with the disintegration process regarding neat PLA. Nevertheless, it was observed that the disintegration rate was reduced with the increasing content of UP resin into PLA rather than being accelerated by the enzymatic attack on the amorphous regions. This reduction in PLA's disintegration rate by adding UP resin could lead to obtaining more durable products to be used in the agriculture sector for mulch film protector [52] and soil sterilization [53], creating the possibility of being reused.

As shown in Fig. 5, from day 21, the mass loss starts to increase due to the scission of the polymer chain caused by the hydrolysis [37], which is remarkably accelerated after day 35. For days 42 and 49, neat PLA shows about 65% and 88% of mass loss, respectively; meanwhile, these percentages were lower for PLA-UP mixtures (e.g. day 42; 47% for PLA-10UP and 31% for PLA-15UP). In addition, at 56 days of incubation, it was observed that neat PLA and PLA samples with the lowest content of UP resin exceeded the 90% disintegration degree required by the ISO 20200. Meanwhile, PLA samples with the highest content of UP resin reached this limit point of disintegration degree after 56 days and later reached 100% of disintegration at 63 days. This low rate of weight loss is attributed to the presence of UP resin on the mixtures, which delays the water diffusion into the material due to its hydrophobic nature as a rosin derivative, thus preventing the hydrolysis of the PLA polymeric

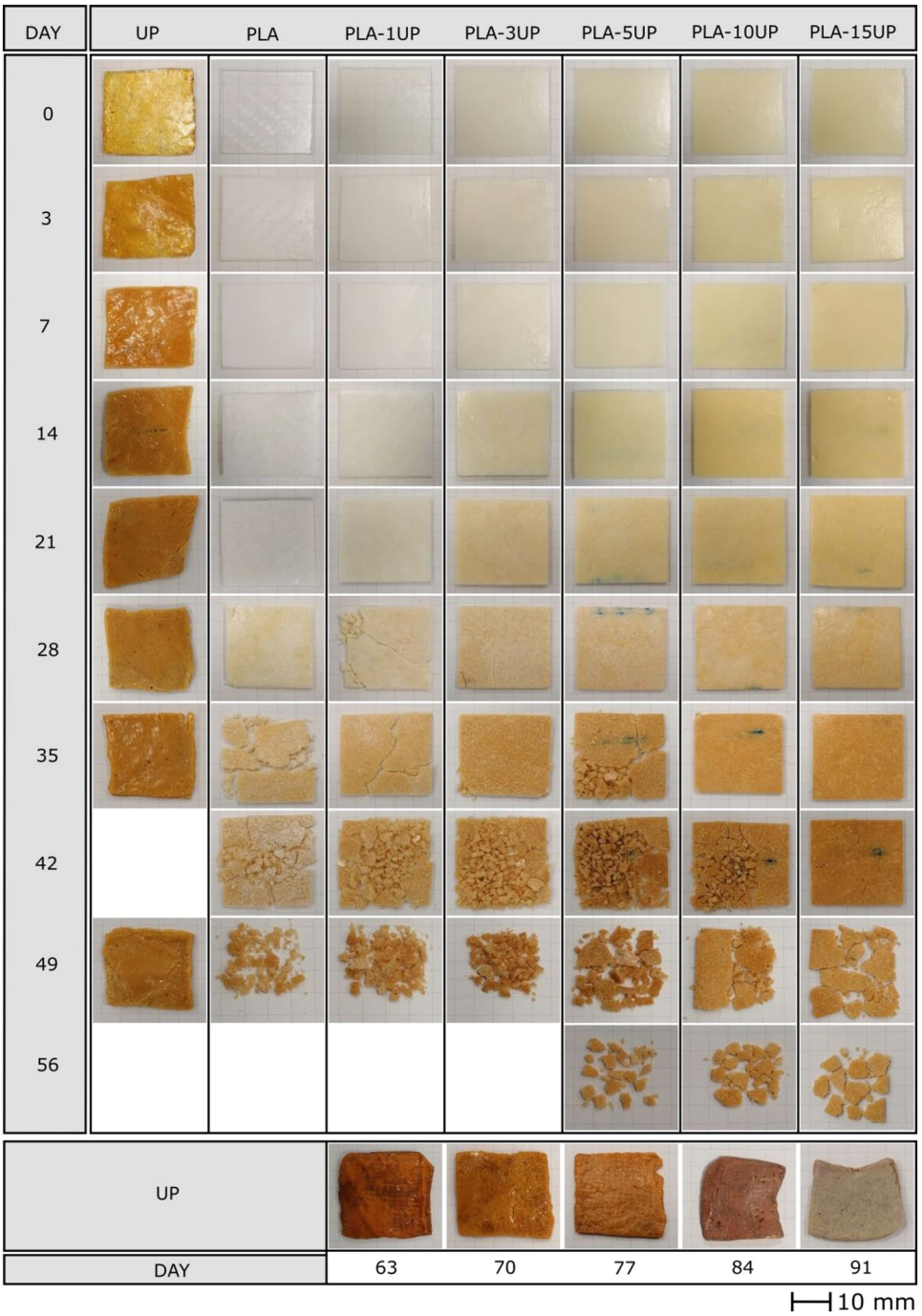

Fig. 4 Visual appearance of UP resin, neat PLA and PLA-UP mixtures after different incubation time under controlled composting conditions

chain. Moreover, it is considered that when the hydrolysis and random chain cleavage of the ester groups are delayed, thus the attack of the microorganisms (present in the composting reactor) on the lactic acid, dimers, and oligomers formed after hydrolysis, is also delayed [54]. As shown in Fig. 5, UP resin was unaffected by the microorganisms in the composting reactor since no variation in the weight of the samples was observed after being extracted throughout the disintegration period (a total of 91 days of incubation). Thus, the hydrophobic and antibacterial characteristics of UP resin are confirmed. Only shape and color changes were observed on UP resin samples (Fig. 4) due to the temperature conditions they were subjected to during the composting process (58 °C). It is considered that the fractions of UP resin, added in the mixtures with PLA, became part of the compost along the disintegration process by breaking down into tiny fragments, which were considered as disintegrated material when sieved, as imposed by ISO 20200. Therefore, no visible residues were observed. Contrary to the disintegration results obtained in this study, Kaavessina et al. [35]

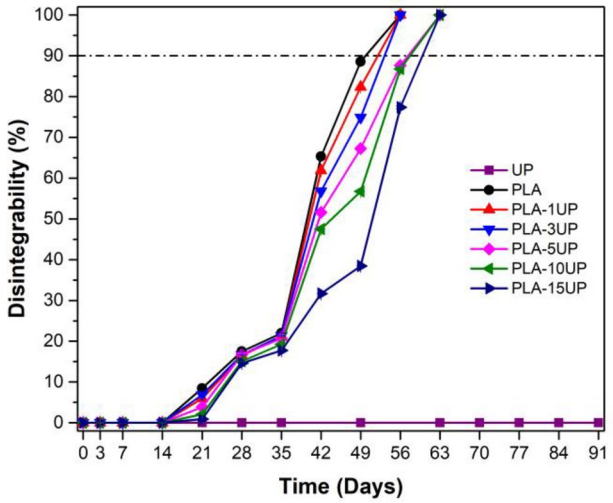

Fig. 5 Degree of disintegration of UP resin, neat PLA and PLA-UP mixtures as a function of incubation time under controlled composting conditions

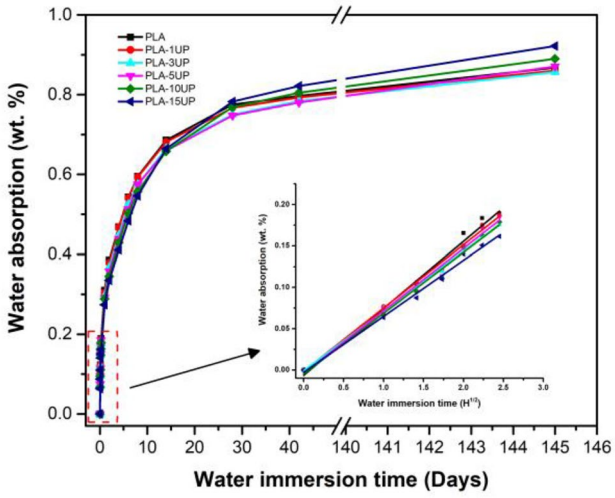

Fig. 6 Evaluation plot of water absorption (wt.%) for neat PLA and PLA-UP mixtures as a function of the immersion time into distilled water at room temperature

have formerly reported an increased degradability rate of PLA by the increasing content of gum rosin (gondorukem). The study stated that gondorukem might be acting as a degradation agent. However, it should be considered that gondorukem is the unmodified solid fraction obtained from the exudated liquid of pine trees after evaporating the volatile component [55, 56]. Unmodified gum rosin is characterized by low thermal and oxidative stability and relatively high susceptibility to biodegradation [57]. On the other hand, UP resin is a chemically modified rosin resin with higher thermal stability and water resentence (hydrophobicity prevents the water diffusion and hydrolysis reaction). Hence, it could be concluded that along with the disintegration test, the degradation behavior for neat PLA and PLA-UP blends was split into fragments. This tendency of PLA to break into small pieces was formerly reported in previous work by studying PLA/PCL blends under composting conditions [25].

Figure 6 shows the graphical evolution of the water absorption (wt.%) for neat PLA and PLA-UP mixtures as a function of the immersion time into distilled water at room temperature. It also shows the water absorption (wt.%) plot versus the square root of immersion time. Such graphical evolution illustrates an obtained water absorption percentage for neat PLA around 0.8% during the trial period, a similar value previously reported in other studies [45]. In this regard, unlike the PLA mixtures with 10 and 15 phr content of UP resin, the PLA-UP mixtures presented lower water absorption values than those obtained for neat PLA, mainly at the first stage of the test, where the increase of water absorption had a linear behavior. For PLA-10UP and PLA-15UP, the amount of water absorbed from day 28 was higher than that shown for neat PLA and the other mixtures. This low rate of water absorption obtained for PLA-UP mixtures regarding neat PLA could be explained due to the high hydrophobic characteristic of UP resin, which hinders the water diffusion into the material, as is confirmed by the values shown in Table 3, where both diffusion coefficient (D) and corrected diffusion coefficient (D_c) values tend to decrease with the increasing content of UP resin added. Neat PLA presented a D_c value of 15.3×10^{-7} mm^2 s^{-1}, in accordance with the previously reported value [42]; meanwhile, with only 1 phr addition of UP resin, the D_c decreases by almost half. This confirms the low disintegration rate under composting conditions (shown in Sect. "Disintegration under controlled composting conditions of PLA-UP mixtures") due to the delayed water diffusion and, therefore, the delayed hydrolysis reaction. On the other hand, the increment of water absorption rate for PLA mixtures with 10 and 15 phr content of UP resin after 28 days is attributed to a capillary action [58] in the PLA matrix caused by UP

Table 3 Diffusion coefficient (D) and Corrected diffusion coefficient (Dc) values for neat PLA and PLA-UP mixtures, estimated from the linear region of the weight gained in the first 10 h, by applying Fick's first law

Samples	(D) ($\times 10^{-6}$) (mm^2 s^{-1})	(D_c) ($\times 10^{-7}$) (mm^2 s^{-1})
PLA	3.33	15.3
PLA-1UP	1.97	9.06
PLA-3UP	1.84	8.36
PLA-5UP	1.78	8.26
PLA-10UP	1.67	7.86
PLA-15UP	1.43	6.63

resin saturation (deeply explained in Sect. "Morphological characterization"). Despite UP resin delaying the entry of water molecules to the polymer chains, over time, water molecules can become lodged in more significant amounts into the internal micro-cracks and empty spaces left by UP saturation. However, it was observed that UP resin (modified rosin) does not increase the water absorption of PLA samples as it does the unmodified gum rosin, as formerly reported in previous work [36].

Mechanical Properties

Figure 7 shows the tensile properties evaluation, and Table 4 shows Charpy's impact energy and harness values of PLA mixture materials with different UP resin contents. As observed, neat PLA was characterized by a tensile strength value of 56 MPa and elongation at break of 5%. After the UP resin addition, tensile strength remains relatively constant at high values (56–57 MPa) from 1 to 3 phr content; meanwhile, the elongation at break slightly increases to 7.6% for up to 3 phr UP resin content. However, the values of tensile strength and elongation at break started to decrease for contents higher than 3 phr of UP resin, which may be associated with a saturation alteration. These saturations act as stress concentrators.

In the case of tensile modulus, this parameter was reduced in all formulations, compared to that shown for the neat PLA (3140 MPa), which is ascribed to an increment of PLA ductility by the UP resin effect in the content of 1 and 3 phr. Nevertheless, for PLA-5UP, a slight increase in modulus is observed due to the saturation of UP resin, which acts as reinforcing loads, slightly stiffening the mixtures. From the 10 phr content of UP resin, the tensile modulus declines again due to the saturation alteration.

These results, along with the increment of the energy absorption value from 30.4 kJ m^{-2} (neat PLA) up to 37.3 kJ m^{-2} in the mixture with 3 phr of UP resin (see Table 4), suggest that the optimal amount of UP resin to achieve optimal performance and good interaction with PLA matrix, as well as retaining the material cohesion and increasing its ability to undergoes plastic deformation, is close to 3 phr content. As UP resin increases, stress concentrations increase, reducing impact energy absorption. No significant change was observed regarding the UP resin effect on PLA hardness since all mixtures show values between 81 and 83.

It is well known that a plasticization effect increases the elongation at break and the impact resistance, but it also tends to reduce tensile modulus and strength. For example, Orue et al. [59] reported that epoxidized vegetal oil (EVO) as a plasticizer significantly improved PLA elongation at break with a remarkable decrease in tensile modulus and strength. Ferri et al. [18] also reported a plasticization effect of PLA by using an epoxy-type plasticizer derived from a

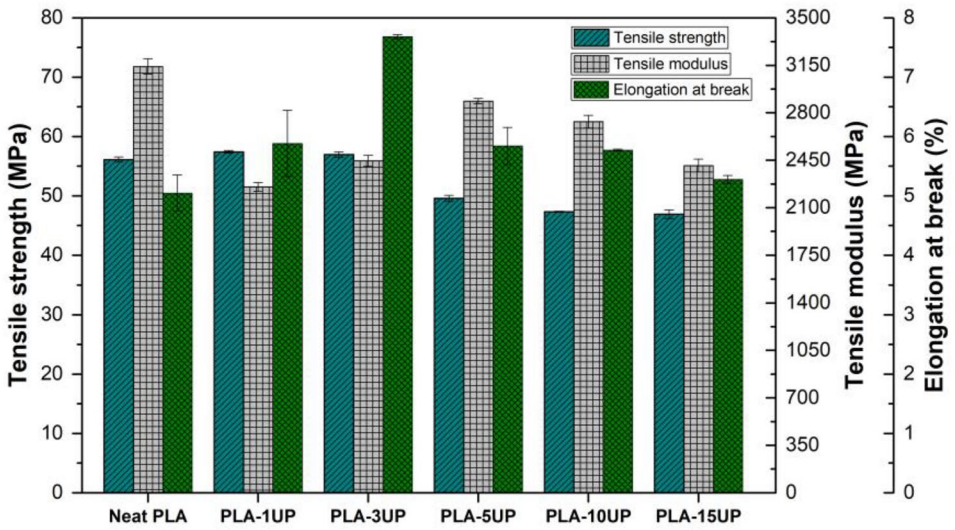

Fig. 7 Tensile properties evaluation of PLA mixture with different UP resin content

Table 4 Charpy's impact energy and hardness values for PLA-UP mixtures in terms of the rosin resin derivative contents

Property	Resin content (phr)					
	0	1	3	5	10	15
Charpy's impact energy (kJ m^{-2})	30.4 ± 0.7	31.1 ± 0.9	37.3 ± 1.0	29.5 ± 1.2	28.5 ± 0.7	24.4 ± 0.4
Hardness (Shore D)	83 ± 0.5	81 ± 0.8	82 ± 0.8	82 ± 0.5	83 ± 0.6	82 ± 0.8

fatty acid, octyl epoxy stearate (OES). The main benefit of OES was the remarkable increase of elongation at break value from below 10% for neat PLA up to 40%. An improvement in the impact-absorbed energy with a percentage increment of 75% was also obtained. Both enhancements were achieved by adding only 5 phr of OES. However, Quiles-Carrillo et al. [7] observed an interesting effect of maleinized hemp seed oil (MHO) on PLA. Beyond obtaining the expected improvement in elongation at break and increased impact-absorbed energy due to the MHO plasticizer, they also reported a noticeable increment in both tensile modulus and strength. They proposed that this behavior could be ascribed to a chain-extension effect provided by MHO due to the possibility that maleic anhydride (MAH) groups present in MHO could react with terminal hydroxyl (–OH) groups of the PLA chains.

In this study, a different effect of UP resin on PLA was observed, which could be attributed to a possible interaction of PLA matrix and the UP resin used due to partial miscibility between components, especially in the mixtures with low content of UP resin. Generally, a partially miscible mixture would obtain intermediate properties to the expected [60].

The dynamic mechanical analysis shows another route to understanding the mechanical properties and the viscoelastic behavior of the neat PLA and PLA-UP mixtures in the analyzed temperature range. The storage modulus (G') and damping factor (tan δ) are shown in Fig. 8. From 60 to 70 °C, an important G′ loss is associated with PLA's chain motions. It is correlated to the glass transition temperature (T_g) of PLA, being through the damping factor (tan δ) peak (Fig. 8b) from where its exact values are obtained. No significant changes in T_g can be observed due to the poor plasticizing effect of the UP resin on PLA. The T_g of PLA and PLA-UP mixtures are similar (around 65 ℃). The low crystallinity percentage of neat PLA is the reason for the significant decrease in G' and the increase of the viscous component during the glass transition process, resulting in a very important softening of the material. Therefore, G' of neat PLA is reduced by up to three orders of magnitude. On the other hand, adding UP resin to PLA results in lower *G values than* neat PLA, including the values obtained in the glass transition process. Only adding 3 phr content of UP resin, G' decreases from 1.31 GPa (neat PLA) to 1.25 GPa (at 40 °C). The higher the UP resin content is, the lower G' values are observed. The tan δ values corresponding to PLA-UP mixtures do not show significant changes to that obtained by neat PLA. However, G' shows differences with the variation of UP resin content, especially for the temperature range between 80 and 110 ℃. The increase of G' in this temperature range is attributed to the crystallization process, which can also be evaluated from the DMTA analysis perspective beyond the DSC test. With only 1 phr content of UP resin added, the beginning of the crystallization process is achieved at lower temperatures regarding neat PLA; meanwhile, for higher UP resin contents, the beginning of the crystallization is achieved at higher temperatures. Therefore, it is confirmed that the UP resin that remains saturated in the PLA matrix acts as a steric hindrance, making the rearrangement of the PLA chains difficult. Finally, adding UP resin to PLA slightly increases the viscous component and decreases the elastic component of the complex modulus, thus showing materials with slightly higher ductility. This is observed for PLA mixtures with low UP resin contents, especially those below the saturation value. However, in general terms, the observed changes in the complex modulus due to the incorporation of UP resin are not significant, as can be seen for other properties studied in this work.

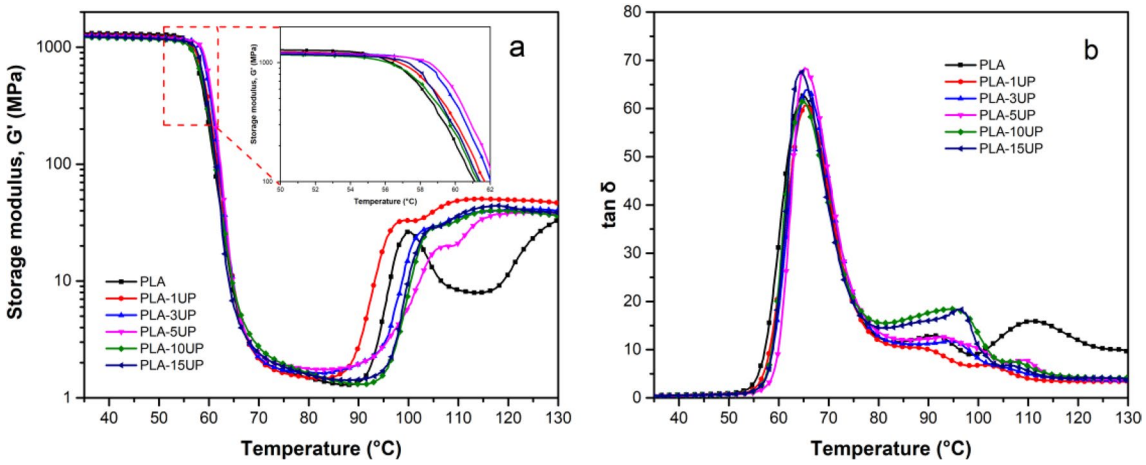

Fig. 8 Comparative evaluation plot of the storage modulus (G′) (**a**) and damping factor (tan δ) (**b**) for PLA and PLA-UP mixtures

Morphological Characterization

The morphology microstructure of neat PLA and PLA-UP mixtures observed by FESEM, shown in Fig. 9, discloses that the PLA mixtures with 1 and 3 phr content of UP resin are completely miscible. Meanwhile, by increasing the UP resin content above 3 phr, the mixtures become immiscible since saturation of UP resin is observed. Figure 9a shows a neat PLA rough surface due to its relative brittleness, characteristic of the quick cracks spread during the impact test. The fractured surface of PLA mixtures containing 1 and 3 phr of UP resin, Fig. 9b and c, respectively, reveal the monophasic structure that evidences the miscibility. In addition, it can be observed some filaments, emphasized with white ovals, in which a detachment of material in a ductile way has occurred. Indeed, the FESEM images suggest that the materials have undergone a significant plastic deformation during the impact test, in accordance with the increment of the impact-absorbed energy values obtained for these mixtures. However, some spherical microdomains began to appear from the 5 phr content of UP resin (Fig. 9d), emphasized with white arrows. In Fig. 9e and f, it can be seen that, as the contents of UP resin increase, the amount of non-homogeneous size spherical microdomains also increases, which are ascribed to the UP resin dispersed into the PLA matrix. Such microdomains are suggested to be

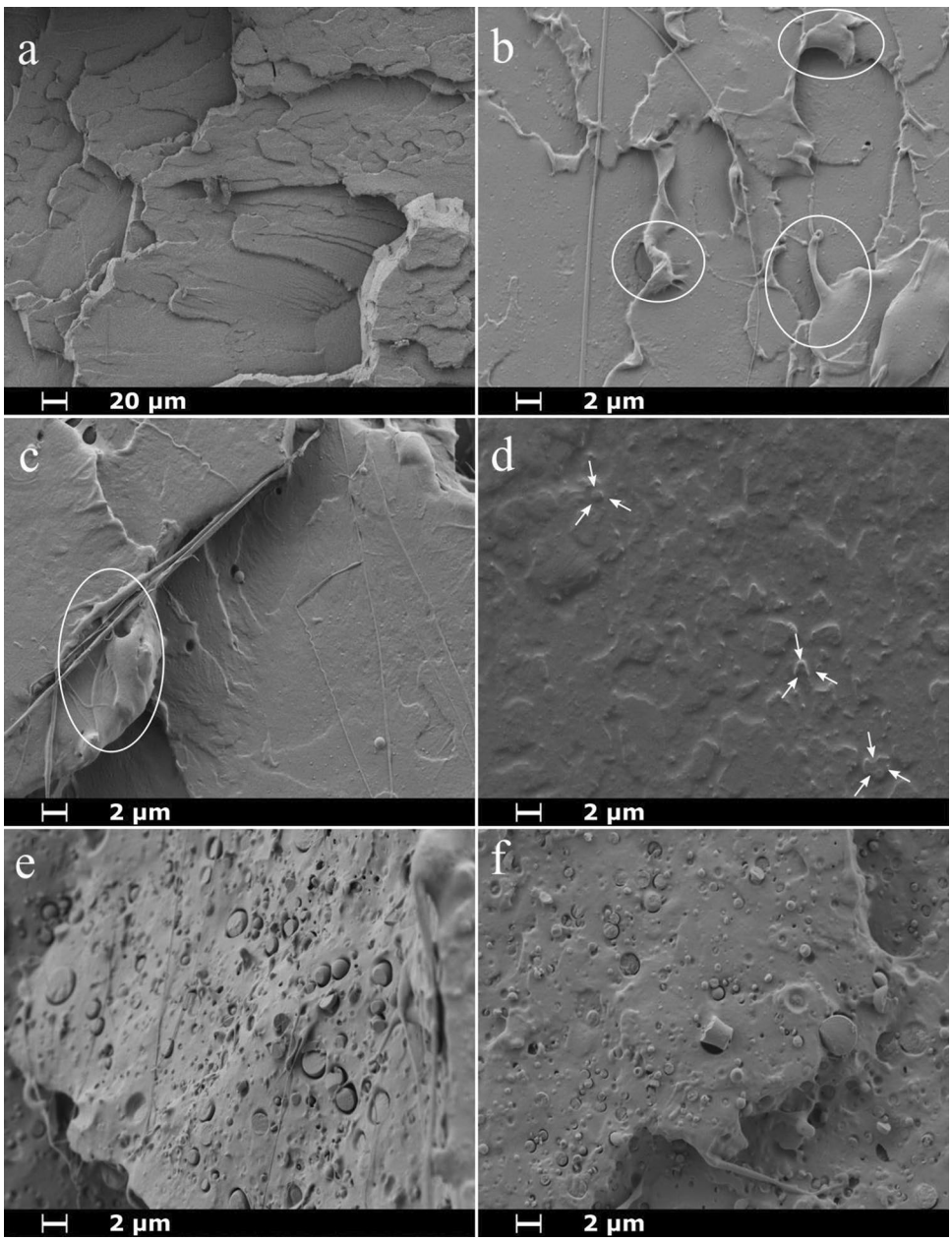

Fig. 9 Cross-section images of impact fracture specimens of the neat PLA and the PLA-UP mixtures, obtained by FESEM: **a** neat PLA at 200×, **b** PLA-1UP at 2000×, **c** PLA-3UP at 2000×, **d** PLA-5UP at 2000×, **e** PLA-10UP at 5000× and **f** PLA-15UP at 5000×

responsible for the mechanical properties decrease in mixtures that contain over 5 phr of UP resin, causing a fragile fracture due to saturation of the UP resin. Similar results have been formerly reported by Aldas et al. [61], who studied binary blends of thermoplastic starch (TPS) and pine resin derivatives. Their studies describe the observation of some micro-voids and micro-domains attributed to the presence of pine resin derivatives in the TPS matrix. These defects are responsible for reducing mechanical resistance and, in some cases, phase debonding [61–63]. In addition, in Fig. 9e and f, almost perfect spherical microdomains surrounded by empty space and some fractured spherical microdomains are also observed. This microstructure suggests that the spherical microdomains are separated from the PLA matrix. Therefore, there has been low miscibility and interfacial adhesion between the UP resin and the PLA polymeric chains. On the other hand, the fractured spherical microdomains are attributed to the saturation of UP, which is a brittle material at room temperature.

Conclusions

Biodegradable materials containing a phenolic-free modified rosin resin (UP) in different content to control the biodegradability of poly (lactic acid) (PLA) under composting conditions were successfully obtained and characterized. It was observed that with the lower UP resin contents (1 and 3 phr), the thermal characteristics remained as that of neat PLA. However, with the increasing content of UP resin, the thermal degradation resistance decreases. UP resin addition promoted higher chain mobility and modified the crystallinity structure of the PLA; thus, the material became more amorphous as UP resin content increased. Moreover, the disintegration rate was reduced with the increasing content of UP resin in PLA due to the hydrophobic and antibacterial characteristics of the UP resin. Also, delaying the water diffusion into the material, thus preventing the hydrolysis of PLA, and the attack of the microorganisms on the PLA. Regarding the mechanical properties, for 1 and 3 phr content, the tensile strength remains similar to PLA values; meanwhile, the elongation at break slightly increases. However, the values of tensile strength and elongation at break started to decrease for contents higher than 3 phr UP, while the tensile modulus was reduced in all formulations. These results are associated with a saturation of the UP resin (for compositions above 3 phr). This behavior, also observed by Charpy's impact and DMA assessment, was confirmed by the study of the microstructure of the materials, where the mixtures with lower contents UP resin were completely miscible and showed a significant plastic deformation during the impact test in good accordance with the increased impact-absorbed energy values obtained for these mixtures. In contrast, for contents above 3 phr, the mixtures become immiscible, and the UP resin's saturation was observed in spherical microdomain shapes. Results suggest that 3 phr is the optimal amount of UP resin to achieve good interaction with the PLA matrix and retain the material cohesion, increasing its ability to undergo plastic deformation.

Acknowledgements H.D.L.R.-R thanks UPV for the grant received through the (FPI-2018-S2-31946) program and the UPV doctoral school for the interchange mobility grant (Resolution. 16/12/21). And UPV authors thank United Resins—Produção de Resinas S.A. (Figueira da Foz, Portugal) for kindly supplying the UP resin and for the collaboration in Project nº E! 114728 "Development and demonstration of innovative bio-resin-based polymers for industrial applications"—DDIBIORESIN (Project EUREKA—EUROSTARS 2).

Author contributions Conceptualization HDR, MA, MDS; formal analysis, HDR, JMF, MDS, FP; funding acquisition JLM, MDS; investigation HRD, MA, JMF, FP; methodology HDR, JMF, FP; project administration JLM, MDS; resources JLM; supervision MDS; validation MA, JMF; visualization HDR, MA, JMF; roles/writing—original draft HDR, JMF; writing—review and editing HDR, MA, MDS.

Funding Open Access funding provided thanks to the CRUE-CSIC agreement with Springer Nature. This research was funded by MCIN/AEI/10.13039/501100011033 through PID-AEI Project (grant PID2021-123753NA-C33 and PID2020-116496RB-C22) and TED-AEI Project (grants TED2021-129920A-C43), and, as appropriate, by "ERDF A way of making Europe", by the "European Union" or by the "European Union NextGenerationEU/PRTR".

Declarations

Conflict of interest The authors declare no competing interests.

References

1. Samper MD, Bertomeu D, Arrieta MP, Ferri JM, López-Martínez J (2018) Interference of biodegradable plastics in the polypropylene recycling process. Materials 11(10):1–18. https://doi.org/10.3390/ma11101886
2. Zhong Y, Godwin P, Jin Y, Xiao H (2020) Biodegradable polymers and green-based antimicrobial packaging materials: a mini-review. Adv Ind Eng Polym Res 3(1):27–35. https://doi.org/10.1016/j.aiepr.2019.11.002
3. Reichert CL et al (2020) Bio-based packaging: materials, modifications, industrial applications and sustainability. Polymers 12(7):1558–1593. https://doi.org/10.3390/polym12071558

4. European Bioplastic (2019) Bioplastics market data 2019. Global production capacities of bioplastic 2019–2024. In: European bioplastic conference, vol. 9, no 1, pp 1–14 [Online]. Available from: https://www.european-bioplastics.org/market/. Accessed 29 Jun 2023
5. Balart JF, Montanes N, Fombuena V, Boronat T, Sánchez-Nacher L (2018) Disintegration in compost conditions and water uptake of green composites from poly(lactic acid) and hazelnut shell flour. J Polym Environ 26(2):701–715. https://doi.org/10.1007/s10924-017-0988-3
6. Elsawy MA, Kim KH, Park JW, Deep A (2017) Hydrolytic degradation of polylactic acid (PLA) and its composites. Renew Sustain Energy Rev 79: 1346–1352. https://doi.org/10.1016/j.rser.2017.05.143
7. Quiles-Carrillo L, Blanes-Martínez MM, Montanes N, Fenollar O, Torres-Giner S, Balart R (2018) Reactive toughening of injection-molded polylactide pieces using maleinized hemp seed oil. Eur Polymer J 98:402–410. https://doi.org/10.1016/j.eurpolymj.2017.11.039
8. Castro-Aguirre E, Iñiguez-Franco F, Samsudin H, Fang X, Auras R (2016) Poly(lactic acid)—mass production, processing, industrial applications, and end of life. Adv Drug Del Rev 107: 333–366. https://doi.org/10.1016/j.addr.2016.03.010
9. Li Z, Ye L, Zhao X, Coates P, Caton-Rose F, Martyn M (2017) Structure and biocompatibility of highly oriented poly(lactic acid) film produced by biaxial solid hot stretching. J Ind Eng Chem 52:338–348. https://doi.org/10.1016/j.jiec.2017.04.008
10. Narayanan M, Loganathan S, Valapa RB, Thomas S, Varghese TO (2017) UV protective poly(lactic acid)/rosin films for sustainable packaging. Int J Biol Macromol 99:37–45. https://doi.org/10.1016/j.ijbiomac.2017.01.152
11. Arrieta MP, Samper MD, Aldas M, López J (2017) On the use of PLA-PHB blends for sustainable food packaging applications. Materials 10(9). https://doi.org/10.3390/ma10091008
12. Auras R, Harte B, Selke S (2004) An overview of polylactides as packaging materials. Macromol Biosci 4(9): 835–864. https://doi.org/10.1002/mabi.200400043
13. Luzi F et al (2019) Combined effect of cellulose nanocrystals, carvacrol and oligomeric lactic acid in PLA_PHB polymeric films. Carbohyd Polym 223(1): 115131. https://doi.org/10.1016/j.carbpol.2019.115131
14. Fortunati E, Luzi F, Puglia D, Petrucci R, Kenny JM, Torre L (2015) Processing of PLA nanocomposites with cellulose nanocrystals extracted from *Posidonia oceanica* waste: innovative reuse of coastal plant. Ind Crops Prod 67:439–447. https://doi.org/10.1016/j.indcrop.2015.01.075
15. Arrieta MP, Sessini V, Peponi L (2017) Biodegradable poly(ester-urethane) incorporated with catechin with shape memory and antioxidant activity for food packaging. Eur Polymer J 94(1):111–124. https://doi.org/10.1016/j.eurpolymj.2017.06.047
16. Huang MH, Li S, Vert M (2004) Synthesis and degradation of PLA–PCL–PLA triblock copolymer prepared by successive polymerization of ε-caprolactone and DL-lactide. Polymer 45(26):8675–8681. https://doi.org/10.1016/j.polymer.2004.10.054
17. Carbonell-Verdu A, Samper MD, Garcia-Garcia D, Sanchez-Nacher L, Balart R (2017) Plasticization effect of epoxidized cottonseed oil (ECSO) on poly(lactic acid). Ind Crops Prod 104(1):278–286. https://doi.org/10.1016/j.indcrop.2017.04.050
18. Ferri JM, Samper MD, García-Sanoguera D, Reig MJ, Fenollar O, Balart R (2016) Plasticizing effect of biobased epoxidized fatty acid esters on mechanical and thermal properties of poly(lactic acid). J Mater Sci 51(11): 5356–5366. https://doi.org/10.1007/s10853-016-9838-2
19. Garcia-Garcia D, Carbonell-Verdu A, Arrieta MP, López-Martínez J, Samper MD (2020) Improvement of PLA film ductility by plasticization with epoxidized karanja oil. Polym Degr Stab 179. https://doi.org/10.1016/j.polymdegradstab.2020.109259
20. Zhao TH, Yuan WQ, Li YD, Weng YX, Zeng JB (2018) Relating chemical structure to toughness via morphology control in fully sustainable sebacic acid cured epoxidized soybean oil toughened polylactide blends. Macromolecules 51(5):2027–2037. https://doi.org/10.1021/acs.macromol.8b00103
21. Ferri JM, Garcia-Garcia D, Carbonell-Verdu A, Fenollar O, Balart R (2018) Poly (lactic acid) formulations with improved toughness by physical blending with thermoplastic starch. J Appl Polym Sci 45751(4):1–8. https://doi.org/10.1002/app.45751
22. Mihai M, Huneault MA, Favis BD, Li H (2007) Extrusion foaming of semi-crystalline PLA and PLA/thermoplastic starch blends. Macromol Biosci 7(7):907–920. https://doi.org/10.1002/mabi.200700080
23. Arrieta MP, López J, Hernández A, Rayón E (2014) Ternary PLA-PHB-Limonene blends intended for biodegradable food packaging applications. Eur Polymer J 50(1):255–270. https://doi.org/10.1016/j.eurpolymj.2013.11.009
24. Iglesias Montes ML, Cyras VP, Manfredi LB, Pettarín V, Fasce LA (2020) Fracture evaluation of plasticized polylactic acid/poly (3-HYDROXYBUTYRATE) blends for commodities replacement in packaging applications. Polym Test 84: 106375. https://doi.org/10.1016/j.polymertesting.2020.106375
25. Ferri JM, Fenollar O, Jorda-Vilaplana A, García-Sanoguera D, Balart R (2016) Effect of miscibility on mechanical and thermal properties of poly(lactic acid)/polycaprolactone blends. Polym Int 65(4):453–463. https://doi.org/10.1002/pi.5079
26. Rao RU, Venkatanarayana B, Suman KNS (2019) Enhancement of mechanical properties of PLA/PCL (80/20) blend by reinforcing with MMT nanoclay. Mater Today Proc 18:85–97. https://doi.org/10.1016/j.matpr.2019.06.280
27. Gere D, Czigany T (2020) Future trends of plastic bottle recycling: compatibilization of PET and PLA. Polym Test 81(1): 106160. https://doi.org/10.1016/j.polymertesting.2019.106160
28. Hachemi R, Belhaneche-Bensemra N, Massardier V (2014) Elaboration and characterization of bioblends based on PVC/PLA. J Appl Polym Sci 131(7). https://doi.org/10.1002/app.40045
29. Boubekeur B, Belhaneche-Bensemra N, Massardier V (2020) Low-density polyethylene/poly(lactic acid) blends reinforced by waste wood flour. J Vinyl Add Technol vnl.21759. https://doi.org/10.1002/vnl.21759
30. Ferri JM, Garcia-Garcia D, Rayón E, Samper MD, Balart R (2020) Compatibilization and characterization of polylactide and biopolyethylene binary blends by non-reactive and reactive compatibilization approaches. Polymers 12(6):1344–1364. https://doi.org/10.3390/POLYM12061344
31. Fogašová M et al (2022) PLA/PHB-based materials fully biodegradable under both industrial and home-composting conditions. Polymers 14(19):4113. https://doi.org/10.3390/polym14194113
32. Kucharczyk P, Pavelková A, Stloukal P, Sedlarík V (2016) Degradation behaviour of PLA-based polyesterurethanes under abiotic and biotic environments. Polym Degrad Stab 129:222–230. https://doi.org/10.1016/j.polymdegradstab.2016.04.019
33. Kalita NK, Sarmah A, Bhasney SM, Kalamdhad A, Katiyar V (2021) Demonstrating an ideal compostable plastic using biodegradability kinetics of poly(lactic acid) (PLA) based green biocomposite films under aerobic composting conditions. Environ Challeng 3: 100030. https://doi.org/10.1016/j.envc.2021.100030
34. Moustafa H, El Kissi N, Abou-Kandil AI, Abdel-Aziz MS, Dufresne A (2017) PLA/PBAT bionanocomposites with antimicrobial natural rosin for green packaging. ACS Appl Mater Interfaces 9(23):20132–20141. https://doi.org/10.1021/acsami.7b05557

35. Kaavessina M, Distantina S, Chafidz A, Utama A, Anggraeni VMP (2018) Blends of low molecular weight of poly lactic acid (PLA) with gondorukem (gum rosin). In: AIP Conference Proceedings, vol. 1931, no. 1, p. 030006. https://doi.org/10.1063/1.5024065
36. de la Rosa-Ramirez H, Aldas M, Ferri JM, Samper MD, Lopez-Martinez J (2020) Modification of poly (lactic acid) through the incorporation of gum rosin and gum rosin derivative: mechanical performance and hydrophobicity. J Appl Polym Sci 49346:1–15. https://doi.org/10.1002/app.49346
37. Valentina I, Haroutioun A, Fabrice L, Vincent V, Roberto P (2017) Tuning the hydrolytic degradation rate of poly-lactic acid (PLA) to more durable applications. In: AIP Conference Proceedings, vol. 1914, no. 1. https://doi.org/10.1063/1.5016801
38. Torres-Giner S, Gimeno-Alcañiz JV, Ocio MJ, Lagaron JM (2011) Optimization of electrospun polylactide-based ultrathin fibers for osteoconductive bone scaffolds. J Appl Polym Sci 122(2):914–925. https://doi.org/10.1002/app.34208
39. Neogi P (1996) Diffusion in Polymers, 1st edn. Marcel Dekkel Inc, New York
40. Gil-Castell O et al (2014) Hydrothermal ageing of polylactide/sisal biocomposites. Studies of water absorption behaviour and physico-chemical performance. Polym Degrad Stab 108:212–222. https://doi.org/10.1016/j.polymdegradstab.2014.06.010
41. Tham WL, Poh BT, Mohd Ishak ZA, Chow WS (2015) Water absorption kinetics and hygrothermal aging of poly(lactic acid) containing halloysite nanoclay and maleated rubber. J Polym Environ 23(2): 242–250. https://doi.org/10.1007/s10924-014-0699-y
42. Le Duigou A, Bourmaud A, Davies P, Baley C (2014) Long term immersion in natural seawater of Flax/PLA biocomposite. Ocean Eng 90:140–148. https://doi.org/10.1016/j.oceaneng.2014.07.021
43. Hu C et al (2017) Comparative assessment of the strain-sensing behaviors of polylactic acid nanocomposites: reduced graphene oxide or carbon nanotubes. J Mater Chem C 5(9):2318–2328. https://doi.org/10.1039/c6tc05261d
44. Tawiah B, Yu B, Yuen ACY, Yuen RKK, Xin JH, Fei B (2019) Thermal, crystalline and mechanical properties of flame retarded poly(lactic acid) with a PBO-like small molecule—phenylphosphonic bis(2-aminobenzothiazole). Polym Degrad Stab 163:76–86. https://doi.org/10.1016/j.polymdegradstab.2019.03.002
45. Quiles-Carrillo L, Montanes N, Garcia-Garcia D, Carbonell-Verdu A, Balart R, Torres-Giner S (2018) Effect of different compatibilizers on injection-molded green composite pieces based on polylactide filled with almond shell flour. Compos B Eng 147:76–85. https://doi.org/10.1016/J.COMPOSITESB.2018.04.017
46. Oliveira M, Santos E, Araújo A, Fechine GJM, Machado AV, Botelho G (2016) The role of shear and stabilizer on PLA degradation. Polym Testing 51:109–116. https://doi.org/10.1016/j.polymertesting.2016.03.005
47. Backes EH, Pires LN, Costa LC, Passador FR, Pessan LA (2019) Analysis of the degradation during melt processing of PLA/biosilicate® composites. J Compos Sci 3(2): 52. https://doi.org/10.3390/jcs3020052
48. Ferri JM, Motoc DL, Bou SF, Balart R (2019) Thermal expansivity and degradation properties of PLA/HA and PLA/βTCP in vitro conditioned composites. J Therm Anal Calorim 138(4):2691–2702. https://doi.org/10.1007/s10973-019-08799-0
49. Liao J, Liu S, Yuan Y, Zhang H (2018) Steric hindrance effect on the thermo- and photo-responsive properties of pyrene-based polymers. New J Chem 42(8):5698–5708. https://doi.org/10.1039/c8nj00136g
50. Robertson GL (2014) Food packaging. In: Encyclopedia of agriculture and food systems. Elsevier, pp 232–249
51. Pantani R, Sorrentino A (2013) Influence of crystallinity on the biodegradation rate of injection-moulded poly(lactic acid) samples in controlled composting conditions. Polym Degrad Stab 98(5):1089–1096. https://doi.org/10.1016/j.polymdegradstab.2013.01.005
52. Akhir MAM, Mustapha M (2022) Formulation of biodegradable plastic mulch film for agriculture crop protection: a review. Polym Rev 62(4):890–918. https://doi.org/10.1080/15583724.2022.2041031
53. Laverde G (2002) Agricultural films: types and applications. J Plastic Film Sheet 18(4): 269–277. https://doi.org/10.1177/8756087902034748
54. Luzi F, Fortunati E, Puglia D, Petrucci R, Kenny JM, Torre L (2015) Study of disintegrability in compost and enzymatic degradation of PLA and PLA nanocomposites reinforced with cellulose nanocrystals extracted from *Posidonia Oceanica*. Polym Degrad Stab 121:105–115. https://doi.org/10.1016/j.polymdegradstab.2015.08.016
55. Soo KW, Azahari B, Poh BT (2016) Effect of magnesium oxide loading on adhesion properties of ENR 25/NBR blend adhesives in the presence of petro resin and gum rosin tackifiers. J Polym Environ 24(4):334–342. https://doi.org/10.1007/s10924-016-0778-3
56. Barton-Pudlik J, Czaja K, Lipok J (2018) Resistance of conifer needle polyolefin composites (CNPCs) against biodecomposition caused by fungi. J Polym Environ 26(3):1179–1193. https://doi.org/10.1007/s10924-017-1024-3
57. Bildik AE, Hubbe MA, Güle ME (2019) Neutral/alkaline sizing of paper with fortified, saponified wood rosin premixed with alum and retained using cationic polymer. Appita J 72(1):41–51. https://doi.org/10.3316/INFORMIT.438309087723225
58. Weitsman YJ (2006) Anomalous fluid sorption in polymeric composites and its relation to fluid-induced damage. Compos A Appl Sci Manuf 37(4):617–623. https://doi.org/10.1016/j.compositesa.2005.05.022
59. Orue A, Eceiza A, Arbelaiz A (2018) Preparation and characterization of poly(lactic acid) plasticized with vegetable oils and reinforced with sisal fibers. Ind Crops Prod 112:170–180. https://doi.org/10.1016/j.indcrop.2017.11.011
60. Balart A, López R, Sánchez J, Nadal L (2001) Introducción a la ciencia e ingeniería de polímeros. Alfagràfic S.A, Alcoy
61. Aldas M, Ferri JM, Lopez-Martinez J, Samper MD, Arrieta MP (2019) Effect of pine resin derivatives on the structural, thermal, and mechanical properties of Mater-Bi type bioplastic. J Appl Polym Sci 137(4):48236. https://doi.org/10.1002/app.48236
62. Aldas M, Pavon C, López-Martínez J, Arrieta MP (2020) Pine resin derivatives as sustainable additives to improve the mechanical and thermal properties of injected moulded thermoplastic starch. Appl Sci (Switzerland) 10(7). https://doi.org/10.3390/app10072561
63. Aldas M, Rayón E, López-Martínez J, Arrieta MP (2020) A deeper microscopic study of the interaction between gum rosin derivatives and a mater-Bi type bioplastic. Polymers 12(1):226. https://doi.org/10.3390/polym12010226